Biochimica et Biophysica Acta 1833 (2013) 2004–2015

Contents lists available at SciVerse ScienceDirect

Biochimica et Biophysica Acta

journal homepage: www.elsevier.com/locate/bbamcr

The FOX transcription factor Hcm1 regulates oxidative metabolism in response to early nutrient limitation in yeast. Role of Snf1 and Tor1/Sch9 kinases

María José Rodríguez-Colman, M. Alba Sorolla, Núria Vall-llaura, Jordi Tamarit, Joaquim Ros, Elisa Cabiscol *

Departament de Ciències Mèdiques Bàsiques, IRBLleida, Universitat de Lleida, Lleida, Catalonia, Spain

ARTICLE INFO

Article history:
Received 20 September 2012
Received in revised form 13 February 2013
Accepted 15 February 2013
Available online 26 February 2013

Keywords:
Forkhead transcription factor
Hcm1
Nutrient limitation
Oxidative metabolism
Snf1 kinase
Yeast

ABSTRACT

Within *Saccharomyces cerevisiae*, Hcm1is a member of the forkhead transcription factor family with a role in chromosome organization. Our group recently described its involvement in mitochondrial biogenesis and stress resistance, and reports here that Hcm1 played a role in adaptation to respiratory metabolism when glucose or nitrogen was decreased. Regulation of Hcm1 activity occurs in at least three ways: i) protein quantity, ii) subcellular localization, and iii) transcriptional activity. Transcriptional activity was measured using a reporter gene fused to a promoter that contains a binding site for Hcm1. We also analyzed the levels of several genes whose expression is known to be regulated by Hcm1 levels and the role of the main kinases known to respond to nutrients. Lack of sucrose-*non*fermenting (Snf1) kinase increases cytoplasmic localization of Hcm1, whereas *Δtor1* cells showed a mild increase in nuclear Hcm1. *In vitro* experiments showed that Snf1 clearly phosphorylates Hcm1 while Sch9 exerts a milder phosphorylation. Although *in vitro*Tor1 does not directly phosphorylate Hcm1, *in vivo* rapamycin treatment increases nuclear Hcm1. We conclude that Hcm1 participates in the adaptation of cells from fermentation to respiratory metabolism during nutrient scarcity. According to our hypothesis, when nutrient levels decrease, Snf1 phosphorylates Hcm1. This results in a shift from the cytoplasm to the nucleus and increased transcriptional activity of genes involved in respiration, use of alternative energy sources, NAD synthesis and oxidative stress resistance.

1. Introduction

All organisms have evolved to respond to changes in environmental conditions. A network of complex signaling pathways ensures the optimum adaptation of cellular metabolism to these fluctuating conditions. Signal transduction components and mechanisms are highly conserved among all eukaryotes. In mammals, hormones (*e.g.*, insulin), growth factors, neurotrophins, nutrients, cytokines, and oxidative stress regulate a family of forkhead transcription factors (FKH-TFs), the forkhead box O family (FoxO). In response to all these stimuli, FoxO factors (FoxO1, 3, 4, and 6) control various biological functions including stress resistance, energy metabolism, DNA repair, cell-cycle arrest, and apoptosis [reviewed in 1–3]. Due to this wide spectrum of functions, FoxO activity is regulated by several posttranslational modifications, such as phosphorylation, acetylation, ubiquitination, methylation, and glycosylation. A complex combination of such modifications regulates FoxO activity by changing its subcellular localization, protein levels, and DNA-binding properties. [2]. Protein–protein interactions between FoxO proteins and their binding partners also have significant consequences on transcriptional activity and other non-canonical FoxO functions, independent of their roles as transcription factors [4,5].

Saccharomyces cerevisiae has four members of the forkhead family of eukaryotic transcription factors (*FKH1*, *FKH2*, *FHL1* and *HCM1*) according to a conserved DNA binding domain [6]. Fkh1 and Fkh2 are involved in transcriptional silencing, cell morphology, and the cell cycle [7–9]. Fhl1 regulates transcription of ribosome-associated proteins [10] and Hcm1 regulates transcription of genes involved in chromosome organization, spindle dynamics, and budding [11]. *HCM1* is periodically transcribed and expressed in late G1 and early S phase, and functions as an S-phase-specific transcriptional activator. Hcm1 is activated by the Swi4/Swi6 complex; once activated, Hcm1 induces transcription of *WHI5*, which represses the Swi4/Swi6 complex in a negative feedback loop [12]. *FKH1*and *FKH2* are among the genes activated by Hcm1. Although chromosome segregation is impaired in the absence of Hcm1, the budding kinetics under optimal growth conditions in *Δhcm1* cells is quite similar to wild-type (WT) cells [12].

In a previous report we demonstrated that Hcm1 is the only yeast FKH-TF that has a dual localization, performing a cytosolic-nuclear shift during the cell cycle [13]. In addition, and like mammalian

Abbreviations: FKH-TF, forkhead transcription factor; FoxO, forkhead box O family; HA, hemagglutinin; PIKK, phosphatidylinositol kinase-related kinase; PI3K, phosphoinositide 3-kinase; ROS, reactive oxygen species; RT-PCR, quantitative real-time PCR

* Corresponding author at: Departament de Ciències Mèdiques Bàsiques, IRBLleida, Universitat de Lleida, Edifici Biomedicina I, Av Alcalde Rovira Roure, 80. 25198 Lleida. Catalonia, Spain. Tel.: +34 973 702 281.
E-mail address: Elisa.cabiscol@cmb.udl.cat (E. Cabiscol).

0167-4889/$ – see front matter © 2013 Elsevier B.V. All rights reserved.
http://dx.doi.org/10.1016/j.bbamcr.2013.02.015

FoxO3, Hcm1 moves to the nucleus upon oxidative stress and this response is positively regulated by Sir2. We also reported a novel role of Hcm1 in mitochondrial metabolism and biogenesis that contributes to stress resistance.

Under conditions of rich media and high glucose concentration, *S. cerevisiae* ferments glucose to ethanol, even though respiration would be energetically more favorable [14]. This phenomenon has been defined as the Crabtree effect. The ethanol excreted to the medium inhibits growth of other micro-organisms, giving yeast cells a competitive advantage. When glucose becomes limiting, yeasts enter the diauxic shift and metabolism changes from glucose fermentation to ethanol respiration, which has been accumulating during the fermentative phase. Finally, when all carbon sources have been exhausted, cells enter the stationary phase (G0). If a different essential nutrient becomes limiting before glucose does, yeast cells directly enter the stationary phase without passing through the diauxic shift.

In yeast, nutrients exert the role that growth factors and hormones play in the regulation of signaling cascades in higher eukaryotes. The constant fluctuation of nutrients has a key role in determining growth, metabolism, stress resistance, and cell cycle. Several nutrient-controlled pathways integrated into a signaling network have been defined in *S. cerevisiae*. A series of well-conserved nutrient sensory protein kinases performs key roles in this signaling network [reviewed in 15].

The main glucose repression pathway is controlled by Snf1 (sucrose-*non*fermenting kinase), the founding member of the AMPK family. This protein kinase is required for transcription of glucose-repressed genes, being necessary for the yeast to adapt to glucose limitation and to utilize alternate carbon sources [16]. Snf1 is also involved in various nutrient-responsive, cell development processes including meiosis, sporulation [14,17], and aging [18]. In addition to its primary role in response to nutrient stress, Snf1 has a role in the cellular responses to other environmental stresses, including oxidative stress [19].

The TOR pathway controls cell growth in diverse eukaryotic organisms. Tor (*t*arget *o*f *r*apamycin) belongs to a conserved group of serine/threonine kinases from the phosphatidylinositol kinase-related kinase (PIKK) family [20,21]. In contrast to most eukaryotes, yeast has two Tor homologues, Tor1 and Tor2. They form two distinct, evolutionary-conserved multimeric protein complexes, TORC1 and TORC2. TORC1 is inhibited under low nitrogen conditions. It regulates nitrogen catabolite-repression, retrograde and stress response, ribosome biosynthesis, autophagy, and growth. On the other hand, TORC2 is rapamycin-insensitive and is thought to regulate the spatial aspects of growth, such as the control of actin polarization [22]. Sch9 is a serine/threonine protein kinase homologous to the mammalian protein kinase B (PKB/AKT), which plays a central role in nutrient-mediated signaling. It is an important downstream component of phosphoinositide 3-kinase (PI3K) signaling. Sch9 has been identified as a Tor substrate and several TORC1-mediated processes involve this kinase [23,24].

This study demonstrates that Hcm1 respond both to glucose and nitrogen deficiency. Main kinases involved in nutrient response pathways (Snf1, Tor1 and Sch9) have been studied as putative regulators of Hcm1 with Snf1 having a preponderant role. The results uncover the role of Hcm1 as involved in adaptation to early nutrient-induced stress conditions by switching from glucose fermentation to aerobic respiration of the sugar. In addition, pathways using alternative energy sources are also activated.

2. Materials and methods

2.1. Yeast strains and growth conditions

The *S. cerevisiae* strains employed in this study are described in Table 1. Standard protocols were used for DNA manipulations and cell transformations [25]. Null mutants were obtained by using the short flanking homology approach after PCR amplification of the *natMX4* cassette in the case of *HCM1*, *SIR2*, *SNF1*, and *TOR1*. The *HCM1*deletion strain was generated in WT strain CML128 [26]. Deletion of *SIR2*, *SNF1* and *TOR1* was performed in MJRC08 strain (CML128 *HCM1-GFP*). Disruption was confirmed by PCR analysis. Overexpression of Hcm1 protein was obtained by replacing the endogenous promoter with a $tetO_7$ promoter as described [27]. Adding the antibiotic repressed expression of the tet construction, resulting in cells with no detectable levels of Hcm1 [13]. The cells were grown at 30 °C by incubation in a rotary shaker using YPD medium containing 1% yeast extract, 2% peptone, 2% glucose, or standard SC medium containing 2% glucose, 0.67% yeast nitrogen base (Difco, without amino acids, ref. 291940), plus 0.14% drop-out mixture (Sigma, ref Y2001) and auxotrophic requirements (0.076 g/l His, 0.38 g/l Leu, 0.076 g/l Trp and 0.076 g/l uracil) [28]. Specific supplements were omitted for selection of the corresponding plasmid-carrying cells. Specific media were prepared to analyze Hcm1 response to nutrients. To analyze the effect of glucose concentration, standard SC medium was prepared with either 0.5%, 2%, or 4% glucose. To analyze the effect of nitrogen concentration, SC medium containing 2% glucose, 0.17% yeast nitrogen base (Difco, without any source of nitrogen, ref. 233520), was prepared with different dropout contents: i) the recommended amount (1× drop-out = 0.14%), ii) half the recommended amount (0.5× drop-out), and iii) twice the recommended amount (2× drop-out). In these experiments, auxotrophic requirements were added, in all cases, twice the standard concentration.

2.2. Plasmids

pCMTR1, pCMSH9 and pCMSF1 were constructed by inserting the entire WT coding gene sequence into pCM262, a derivative of pCM190 [29,30] kindly provided by E. Herrero (University of Lleida, Spain). The gene (*TOR1*, *SCH9*, or *SNF1*) fragments were PCR amplified from CML128 using iProof High-Fidelity DNA Polymerase and hybrid primers containing PstI and NotI restriction sites (Table 2). The resulting PCR product was cloned into pCM262, previously digested with NotI and PstI. The ligation product obtained was used for DH5α transformation followed by selection based on ampicillin resistance. Purified plasmids from positive DH5α were used for yeast strain CML128 transformation, followed by selection for uracil auxotrophy. The plasmids encode either *TOR1*, *SNF1*, or *SCH9* carboxy terminally fused to three hemagglutinin

Table 1
Yeast strains used in this study.

Strain	Relevant genotype	Comments	Source
CML128	*MATaura3-52 his4 leu2-3,112 trp1*	Wild type	[26]
GRB2405	CML128 *HCM1-3HA::natMX4*	Chromosomal *HCM1* tagged with 3HA using the *natMX4* cassette	[13]
MJRC05	CML128 *hcm1::natMX4*	*HCM1* disruption with *natMX4* cassette	[13]
MJRC07	GRB2405 *tetO7-HCM1-3HA::kanMX4*	Integration of $tetO_7$-regulatable *HCM1-HA* in GRB2405	[13]
MJRC08	CML128 HCM1-GFP:: kanMX4	Chromosomal *HCM1* tagged with GFP using the *sGFP-ADH1t-kanMX4* cassette	[13]
MJRC17	MJRC08 *tor1::natMX4*	*TOR1* disruption with *natMX4* cassette in MJRC08	This study
MJRC18	MJRC08 *snf1::natMX4*	*SNF1* disruption with *natMX4* cassette in MJRC08	This study
MJRC26	GRB2405 [psH144/hcm1bs]::URA3.	*WHI5* HCM1:lacZ reporter construct in GRB2405	This study
MJRC27	MJRC05 [psH144/hcm1bs]::URA3.	*WHI5* HCM1:lacZ reporter construct in MJRC05	This study

(HA) tags and one His_6 tag, under transcriptional control of the tet promoter. Their authenticity was verified by restriction mapping of the plasmid. Western blot using anti-HA and anti-His antibodies was used to check that the full-length tagged protein was produced in yeast. HA-Snf1 and HA-Snf1K84R were expressed from pSK119 and pSK120, which contain the wild-type and K84R dead-mutant *SNF1*, respectively [31]. Plasmids pSK119 and pSK120 were kindly supplied by M. Carlson (Columbia University, NY, USA).

2.3. Hcm1 transcriptional activity

The *WHI5* HCM1:lacZ reporter construct, pSH144/hcm1bs, was kindly provided by Dr. L. Breeden (University of Washington, USA). The plasmid contains the Hcm1 binding site sequence obtained from *WHI5* promoter [12]. StuI digestion was performed for plasmid linearization and it was integrated at *URA3* locus to background strains GRB2405 and MJRC05. β-Galactosidase assays were performed to analyze Hcm1 activity. Transformed cells (MJRC26 and MJRC27 strains) were treated as indicated and then collected for protein extraction. Total protein extraction was obtained by mechanical disruption followed by centrifugation and protein levels were measured using the Bradford method. β-Galactosidase activity was measured using a 96-well kinetic assay as described [32]. The reaction rate was assayed over a span of 10 min. Specific activity is defined as $nmol.min^{-1}.mg^{-1}$ protein.

2.4. Western blot analysis

To detect Hcm1-HA and actin, cell extracts were obtained as described [33], separated in SDS-PAGE, and transferred to polyvinylidene difluoride membranes. Anti-HA (1:2500 dilution, from Roche, ref. 1-867-423) and anti-actin (1:2000 dilution, from Chemicon, ref. MAB1501R) were used as primary antibodies. To detect endogenous Snf1 and its activation state, as well as the phosphorylation state of Hcm1, cell extracts were performed as described [34]. In brief, a cell volume corresponding to 2.0 OD_{600} was taken at different culture densities, and boiled in a glass tube for 3 min. After air-cooled, cells were harvested by centrifugation at 3000 ×*g* for 5 min. Each pellet was resuspended in 150 μl 10 mM Tris–HCl, 1 mM EDTA, pH 7.5, plus 150 μl 0.2 M NaOH. After 5 min, the tubes were spun down in a microfuge at 10,000 ×*g* for 1 min. The supernatants were aspirated and the pellets were gently resuspended in 60 μl of SDS-PAGE loading buffer and boiled for 5 min. Samples were cleared by centrifugation at 10,000 ×*g* for 5 min and loaded on SDS-PAGE at 8 μl/lane. Anti-phospho-Thr172-AMPK (1:1000 dilution, Cell Signaling Technology ref. 2531) and anti-polyHistidine (1:1000 dilution, Sigma ref 1029) antibodies were used to detect phospho-Thr210-Snf1 and total Snf1, respectively. Anti-HA was used to detect Hcm1-HA as described above. Immunodetection was performed using the SNAP i.d.TM system (Millipore). The secondary antibodies conjugated to horseradish peroxidase were used as follows: goat anti-mouse antibody (1:40,000 dilution, from Pierce, ref. 31430), goat anti-rabbit antibody (1:40,000 dilution, from Pierce, ref. 31460), and goat anti-rat (1:4000 dilution, from Molecular Probes, ref. A10549). Images were acquired in a ChemiDoc XRS System (Bio-Rad) and analyzed with Quantity One software (Bio-Rad).

2.5. Gene expression analysis

Microarray analysis was performed at the genomic facilities at the Universitat Autònoma de Barcelona as described [35]. Quantitative real-time PCRs (RT-PCR) were performed using the TaqMan System (Applied Biosystems). Total RNA was extracted using the RNeasy kit (Qiagen, ref. 74104) according to the manufacturer's instructions and 1 μg total RNA from each sample was converted into cDNA with 50 ng utilized for each individual RT-PCR assay in a 48-cycle, three-step PCR reaction using the iCycler (Bio-Rad). Amplification was performed using the TaqMan Universal PCR Master Mix kit (Applied Biosystems, Cat. 4304437). Quantification was completed using iCycler IQ Real-Time detection system software (version 2.3, Bio-Rad). For all gene expression analysis, actin (*ACT1*) was used as an internal control. Data represents three technical repeats of each analysis.

2.6. Microscopy studies

To analyze Hcm1 cellular localization under different conditions, *HCM1-GFP*-labeled cells were analyzed by fluorescence microscopy (Olympus DP30 BW) using 488-nm laser excitation for GFP. Pictures were taken and the number of cells with an absence of nuclear stain was counted with ImageJ 1.42b software and represented as a percentage of the total. The cells showing either exclusively nuclear and both nuclear and cytoplasm localization were grouped and indicated as nuclear. Approximately 5% of the cells showed very low fluorescent levels and were removed from the statistics. All of the quantitative values represent averages from three independent experiments with at least 100 cells/experiment.

2.7. Kinase assay

In vitro kinase assays were performed using recombinant Hcm1 and purified kinases. Hcm1-His_6 recombinant protein was obtained from *Eschericha coli* transformed with pCASa-HCM1-10-7. The plasmid-encoding Hcm1 carboxy terminally fused to His6 tag was obtained from Biomedal (Spain). Hcm1-His_6 protein was purified from DH5α cells using a Ni-column (Qiagen, ref. 30600) and served as substrate for *in vitro* kinase assays. Identity of purified Hcm1 was confirmed by MALDI-TOF spectrometry with a 60% coverage (Proteomic facility, CSIC/Universitat Autònoma de Barcelona). Full-length kinases as well as a series of proteolytic products were purified from *S. cerevisiae* and used as enzymes for *in vitro* kinase assays. Pull-down with HA-agarose (Roche, ref. 11815016001) was used to purify the HA-tagged kinases. For kinase assays, purified Hcm1 and kinases were used in a relationship of approximately 1:10. Reaction buffer consisted of 20 mM Hepes pH 7.5, 0.5 mM DTT, 0.5 mM EDTA, 5 mM $MgCl_2$, and 2.5 mM glycerol phosphate. Reactions were incubated for 45 min at 30 °C in a final volume of 20 μl in the presence of 10 μCi of [γ-^{32}P]ATP and 5 μM of "cold" ATP. The reaction products were separated by SDS-PAGE and the phosphorylated proteins were analyzed by blot detection of gamma

Table 2
Plasmids used for protein kinase purification.

Plasmid ID.	Gene	Primers	Fragment size (bp)
pCMTR1	*TOR1*	1. ATTCA*GCGGCCGC*TGATATGGAACCGCATGAGGAGCAG 2. TACTA*CTGCAGC*CAGAATGGGCACCATCC	7413
pCMSH9	*SCH9*	1. ATTCA*GCGGCCGC*CAATATGATGAATTTTTTTACATC 2. TACTA*CTGCAG*TATTTCGAATCTTCCACTGA	2475
pCMSF1	*SNF1*	1. ATTCA*GCGGCCGC*CAACATGAGCAGTAACAACAACAC 2. TACTA*CTGCAGA*TTGCTTTGACTGTTAACGG	1902

1. Primer forward, 2. primer reverse. Sequences in italics represent restriction sites for NotI and PstI in primers 1 and 2, respectively.

radiation. Autophosphorylation assays were performed in the same way without substrate.

2.8. Analysis

Cell growth was monitored in 1-ml cultures in 24-well plates incubated at 30 °C and constant agitation in a PowerWave XS microplate spectrophotometer (Biotek). Plates were sealed with Breathe Easy membranes (Diversified Biotech, USA). Optical density (OD_{600} nm) was recorded every 30 min. Generation times were calculated using Gen5 data analysis software and Microsoft Excel. To analyze the effect of rapamycin, cell cultures at $OD_{600}=0.5$ were treated with 100 nM rapamycin and aliquots were taken at various times. The percentage of cells with either nuclear or cytosolic Hcm1-GFP localization was quantified as described above. Statistical analysis was performed using Student's *t* test.

3. Results

3.1. Role of Hcm1 throughout the growth curve

Hcm1 is involved in mitochondrial metabolism and stress resistance [13]. In our study, several genes needed to activate respiratory metabolism, such as *ADR1* (coding a transcriptional activator involved in the expression of genes that are regulated by glucose repression), were upregulated in Hcm1-overexpressing cells (Supplemental Table S1). These results suggested a role of Hcm1 in adapting to nutrient scarcity. To get further insight into the physiological role of Hcm1, western blot anti-HA was performed using WT (*HCM1-HA*) cells at different culture densities. There was a peak in Hcm1 levels, which increased 3.5-fold, when culture density reached $OD_{600}=3$ (Fig. 1A and B). At this point, glucose concentration in the media was approximately 50% of the initial concentration. A similar profile was observed when *HCM1* gene expression was measured by RT-PCR (Fig. 1C) and, as expected, mRNA levels peak earlier ($OD_{600}=2$) than protein levels. Moreover, using the GFP-tagged Hcm1 strain, localization of the transcription factor was also evaluated. It is interesting to note that when Hcm1 levels were higher, nuclear translocation increased (Fig. 1D and E). This was a transient response since both Hcm1 levels and nuclear localization decreased at higher culture densities. Growth curves in YPD were obtained from WT, *Δhcm1* and Hcm1-overexpressing (*tetHCM1-HA*) cells (Fig. 2A). In rich medium, *Δhcm1* stopped growth sooner and reached lower densities than WT cells. In contrast, cells overproducing Hcm1 were better fitted for diauxic shift and yielded higher culture densities than WT cells. Although in WT cells the diauxic shift can be observed around $OD_{600}=$ 10–11 (Fig. 2A), metabolic changes started earlier. In fact, when plotted in a logarithmic scale, it is clear that the culture did not grow exponentially beyond $OD_{600}=5$ (Fig. 2B). Such metabolic changes are induced by master kinases like Snf1. As can be seen in Fig. 2C, activation of Snf1, detected by its phosphorylation state, started as early as $OD_{600}=2$ and reached a maximum around $OD_{600}=4$–5.

These results indicate an important role for Hcm1 as an early regulator of nutrient deficiency. Thus, when glucose (or another important nutrient such as nitrogen) becomes scarce, Hcm1 is upregulated and translocated to the nucleus, triggering a response to adapt the cells to the new situation. To examine the role of Hcm1 along the growth curve, several genes known to be induced in Hcm1-overexpressed cells [13] were measured by RT-PCR in WT and *Δhcm1* cells (Fig. 3). As shown, the absence of the transcription factor results in a lower induction in almost all genes tested. Differences between WT and *Δhcm1* strains were especially important in *HSP26* (response to stress) and *PUT1* (use of proline as energy source), which showed almost no induction when Hcm1 was absent. *ADR1* (activation of respiratory genes), along with *BNA2* and *BNA4* (NAD biosynthesis), also presented greatly reduced induction in *Δhcm1* compared to WT strain.

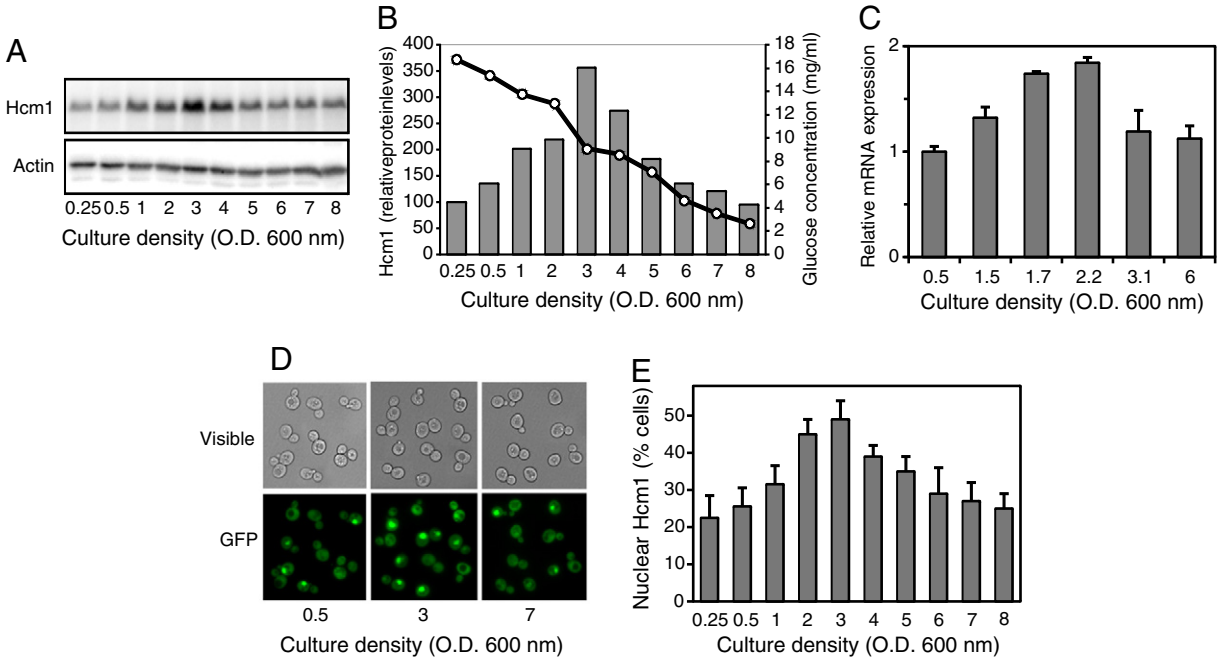

Fig. 1. Hcm1 shows increased protein amount, nuclear localization, and mRNA levels at early stages of nutrient depletion. A. *HCM1-HA* cells were grown with YPD and Hcm1 levels were analyzed by western blot with anti-HA antibodies. Actin was used as a loading control. B. Bands corresponding to Hcm1 in A were measured with a densitometer and the relative intensities were calculated. The data represented an average experiment. Remaining glucose concentration in the extracellular medium was also measured at each culture density (line with open circles). C. WT cells were grown in YPD and expression of *HCM1* was determined by quantitative real-time PCR analysis. Actin expression was used as an internal control to normalize expression levels. D. *HCM1-GFP* cells were grown in YPD and pictures were taken by fluorescent microscopy at three culture densities. E. Percentage of cells showing nuclear localization along the growth culture was quantified. The data are represented as the means ± SD from two experiments with three technical repeats.

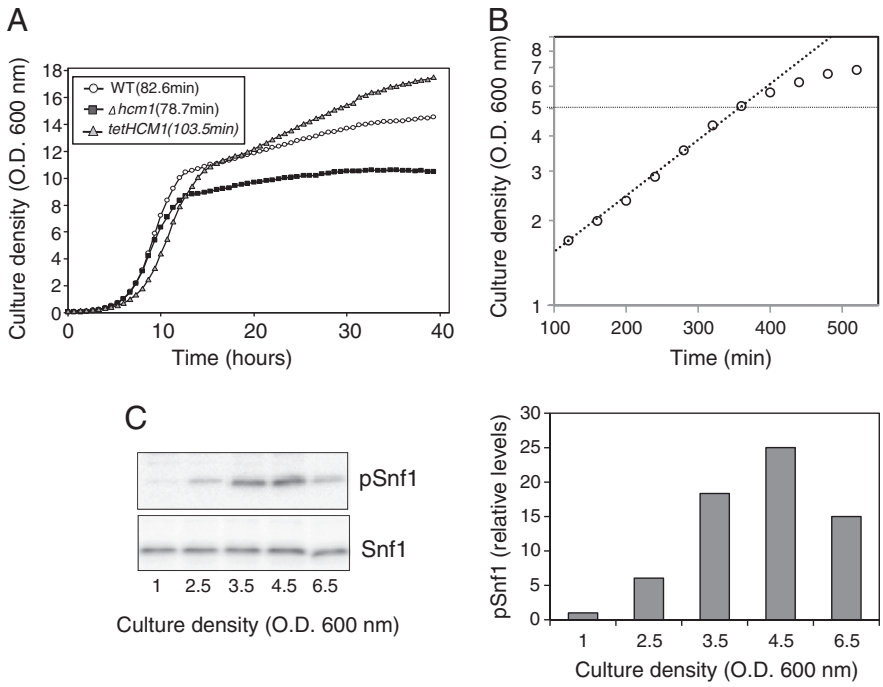

Fig. 2. Effect of Hcm1 levels on cell density and metabolic change measured by generation time and Snf1 activation. A. Growth curves of WT, *Δhcm1* and *tetHCM1* were measured when grown in YPD medium. Duplication time was obtained at the exponential phase. The data are the averages of two independent experiments. B. Logarithmic representation of WT cells grown in YPD. C. WT cells were grown with YPD and pSnf1 and total Snf1 levels were analyzed by western blot with anti-pAMPK and anti-polyHis antibodies, respectively. Bands of pSnf1 were quantified, normalized by total Snf1 levels, and the relative intensities of pSnf1 are indicated in a bar chart. The data represents an average experiment.

3.2. Hcm1 is induced and activated both by glucose and nitrogen deficiency

In a yeast culture, when the cell density increases nutrients begin to be present in limiting amounts. To see whether Hcm1 responds to decreased levels of either glucose or nitrogen, media with different amounts of such components were used (see Materials and methods). Hcm1 levels were measured at different culture densities (Fig. 4A and B). From these experiments it is clear that the peak of Hcm1 expression varies according to both glucose and nitrogen concentrations. After a shift from 2% glucose to 0.5% glucose media, Hcm1 translocated to the nucleus transiently (Fig. 4C). Similarly, when the percentage of cells with nuclear Hcm1-GFP in three media with different nitrogen concentrations was measured, nuclear translocation parallels to Hcm1 expression throughout the growth of the culture (Fig. 4D). Of note, the rate of glucose consumption showed no differences between these three media, up to OD_{600}~8 (not shown).

To measure the transcriptional activity of Hcm1, the promoter of *WHI5* (a gene known to be regulated by Hcm1), fused to LacZ [12] was used. Beta-galactosidase activity was measured under various conditions as a reporter of Hcm1 transcriptional activity. Increased levels of β-galactosidase activity were observed when cells were shifted from 2% to 0.5% (or 0.1%) glucose growth medium (Fig. 5A). Similar results were obtained when cells were shifted from high to low nitrogen content in the culture media (Fig. 5B). As a negative control, β-galactosidase activity was measured in a *Δhcm1* strain having less than 20% of the WT strain's activity.

3.3. Regulation of Hcm1 by nutrient-sensory protein kinases

In yeast, as in mammals, several pathways have been described to be activated either by glucose or nitrogen limitation, and a few master kinases play a key role. In mammals, it is known that FoxOs are regulated at multiple phosphorylation sites, each one having a particular role [reviewed in 36]. In this context, we analyzed the role of three kinases, Tor1 (PIKK family), Snf1 (AMPK family) and Sch9 (PKB/AKT family). To that end, cellular localization of Hcm1-GFP was analyzed in *Δtor1* and *Δsnf1* cells grown exponentially (Fig. 6A). The deletion strain of *SCH9* could not be obtained in our WT background, probably due to the high genetic instability of this mutant. The more clear phenotype was observed in cells lacking Snf1, where Hcm1-GFP was present mainly in the cytoplasm (75% of the cells). Lack of Tor1 slightly favored nuclear Hcm1 localization. The ratio between the percentage of cells with cytosolic *versus* nuclear Hcm1 localization was 1.85, 3, and 1.38 in WT, *Δsnf1*, and *Δtor1*, respectively, indicating the preponderant role of Snf1 in regulating Hcm1 localization. Nevertheless, the role of the TORC1 pathway on Hcm1 is not negligible, since the addition of rapamycin to the culture caused a nuclear import in up to 50% of Hcm1-GFP after 20 min (Fig. 6B). To study whether these kinases have any role in the transient import of Hcm1 to the nucleus observed in WT cells at OD600 = 3, Hcm1-GFP localization was followed at three different culture densities in *Δtor1* and *Δsnf1* cells (Fig. 6C). As it can be observed, lack of either Tor1 or Snf1 abolished the Hcm1 response to nutrient decrease. Moreover, *Δsnf1* cells grew slowly and did not reach high culture densities.

The effects described above could be explained by a direct phosphorylation of Hcm1, or through an indirect effect. To that end, *in vitro* phosphorylation assays were carried out (Fig. 7). HA-tagged Tor1, Snf1, and Sch9 were purified from yeast and recombinant His_6-tagged Hcm1was purified from *E. coli* (Fig. 7A). Identity of the purified proteins was confirmed by mass spectrometry (not shown). Radioactive-labeled ATP was used to perform the kinase assays (see Materials and methods). The results showed that Snf1 (purified from two different plasmids) phosphorylated Hcm1 (Fig. 7B). To demonstrate the specificity of Hcm1 phosphorylation by Snf1, the kinase assay was also performed with a dead-mutant Snf1 (K84R). As expected, no phosphorylation signal on Hcm1 was observed. These results show that the Snf1 protein kinase activity is required for phosphorylation of the Hcm1. Moreover, they rule out the possibility of Hcm1 phosphorylation by an unknown kinase copurified with Snf1. In our *in vitro* assay, Hcm1 was also phosphorylated by Sch9, but Tor1 did not phosphorylate Hcm1 directly (Fig. 7C). With the exception of Tor1, all these kinases have autophosphorylation activity. Phosphorylation of Snf1-K84R could be

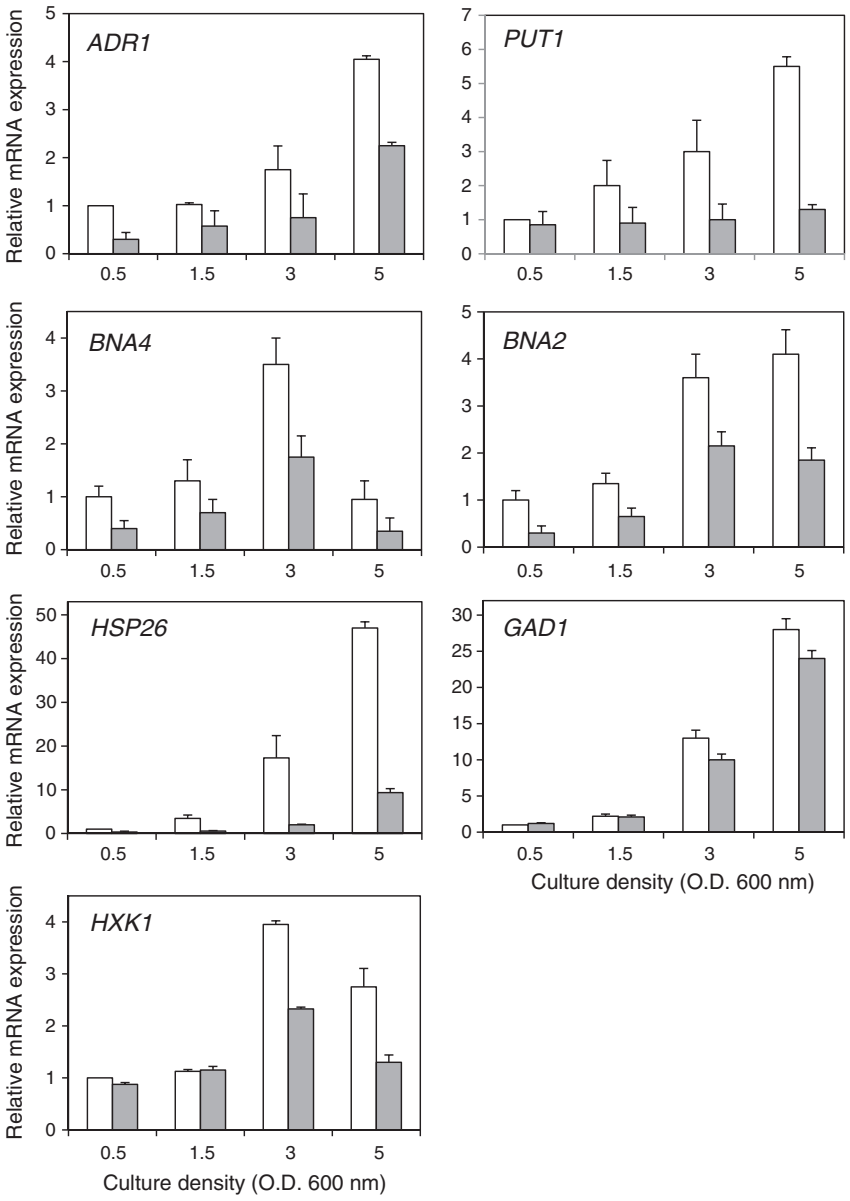

Fig. 3. Role of Hcm1 in the expression of several genes throughout the growth curve. WT and *Δhcm1* cells were grown in YPD and, at different cell densities, expression of several genes was determined by quantitative real-time PCR analysis. Actin expression was used as an internal control to normalize expression levels. White bars, WT strain; gray bars, *Δhcm1* strain. For the WT strain, the relative quantity at $OD_{600} = 0.5$ was set to 1. The data are represented as the means ± SD from two experiments with three technical repeats.

detected only after long exposure times (Supplemental Fig. S1). To check whether Tor1 was purified as an active kinase, *in vitro* phosphorylation assays of Sch9 by Tor1 were performed (Fig. 7D). As shown, in addition to the autophosphorylation activity of Sch9, increased phosphorylation can be detected when Tor1 was present in the assay. This seems to indicate that Tor1 was purified as an active kinase and also that Sch9 is a substrate of Tor1 [23]. Thus, we suggest that Sch9 phosphorylation of Hcm1 could explain the effect of the TORC1 pathway on Hcm1 regulation. However, we cannot rule out that the increased incorporation of ^{32}P detected in Sch9 pull down when mixed with the Tor pull down is due to Sch9 phosphorylation of a substrate present in the TOR preparation.

Phosphorylation of Hcm1 was also observed *in vivo* (Fig. 7E) using a method for protein extraction from boiled cells [34]. The method, described initially to detect phosphorylated Snf1, has the advantage that avoids dephosphorylation by phosphatases present in the cell extract. The results of western blot anti-HA showed extra bands compatible with several degrees of phosphorylated Hcm1. Treatment with alkaline phosphatase confirmed that such modification was due to phosphorylation.

Based on all these results plus data from Table 3 and Supplemental Table S1, the proposed mechanism is summarized in Fig. 8. According to this model, Hcm1, like mammalian FoxOs, would be regulated by phosphorylation at different sites. Phosphorylation of Hcm1 by Snf1 would induce nuclear translocation of the transcription factor, inducing the respiratory metabolism when nutrients decrease. On the contrary, phosphorylation of Hcm1 by Tor/Sch9 at high glucose concentration would promote Hcm1 nuclear export, repressing its transcriptional activity. Taken together, our results suggest that Snf1 is the preponderant Hcm1 regulator.

4. Discussion

Hcm1 was classically described as a cell-cycle transcription factor involved in several aspects of chromosome segregation during the G1/S transition [11,12]. Recently, we described a new role of this

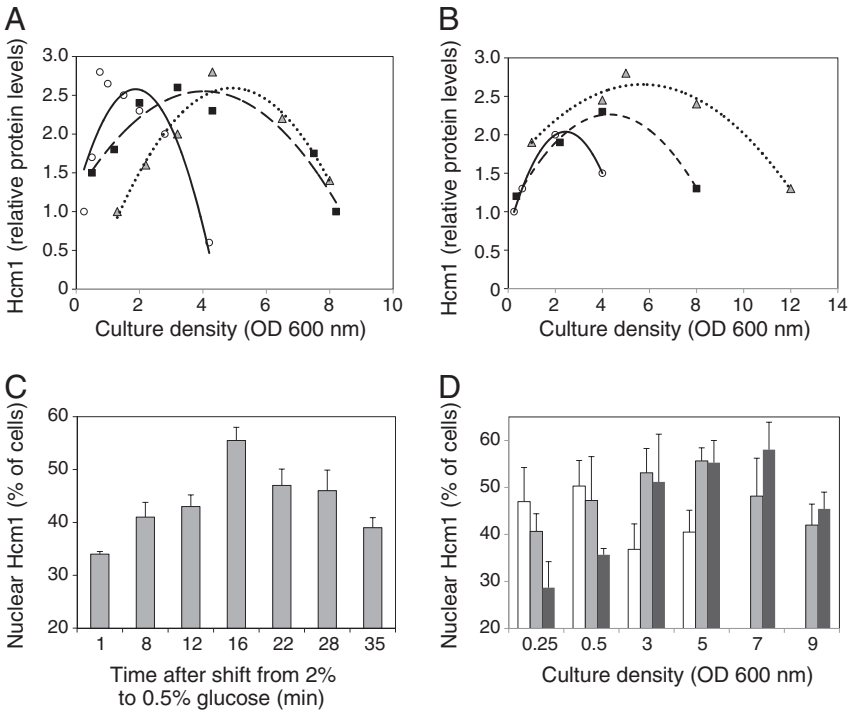

Fig. 4. Hcm1 protein levels and nuclear localization changes when both glucose and nitrogen levels decrease. A and B. *HCM1-HA* cells were grown in the indicated medium at different cell densities and the amount of Hcm1 was measured with western blot anti-HA antibodies: A. SC medium with 0.5% glucose (open circles), 2% (closed squares) and 4% glucose (gray triangles). Hcm1 values are relative to the amount of Hcm1 obtained by western blot at $OD_{600} = 0.25$ with 0.5% glucose (open circles), which was set to 1. B. SC medium without any source of nitrogen and supplemented with drop-out according to the manufacturer's indication (1× drop-out concentration, closed squares), half concentration (0.5× drop-out, open circles), and double concentration (2× drop-out, gray triangles). Hcm1 values are relative to the amount of Hcm1 obtained by western blot at the $OD_{600} = 0.25$ with 0.5× drop-out (open circles), which was set to 1. In A and B, actin was used to normalize protein levels. C. *HCM1-GFP* cells were grown in SC with 2% glucose and at time zero ($OD_{600} = 0.5$) cells were centrifuged and resuspended in SC medium with 0.5% glucose. Pictures were taken at different time points after changing the medium and percentage of cells with nuclear Hcm1 quantified. D. *HCM1-GFP* cells were grown in minimal medium without nitrogen, supplemented with 0.5× drop-out (open bars), 1× drop-out (gray bars) or 2× drop-out (black bars). At different cell densities, images were taken and % of cells with nuclear Hcm1 localization was analyzed. Data are represented as means ± SD from three independent experiments.

TF-inducing mitochondrial metabolism and oxidative stress resistance [13]. Such metabolic change is important to adapt yeast cells to a decreased nutrient availability. Our results demonstrate that the total amount of Hcm1 varies 3- to 4-fold in the exponential phase, reaching the highest value when the glucose concentration is about half of the initial value (around $OD_{600} = 3$ in YPD medium). The amount then drops to basal levels and is almost undetectable in stationary phase (not shown). The increased amount of Hcm1 also parallels a higher percentage of nuclear localization and is preceded by *HCM1* induction. All these events can be envisaged as a preparation for the diauxic shift, since in this phase cells change from fermentative to respiratory metabolism. In fact, cells lacking Hcm1 are unable to enter a diauxic shift, in contrast to WT cells. Cells overexpressing Hcm1 are the best fitted for the transition to diauxic shift and, as a consequence, yield higher culture densities. How can this phenotype be explained? From the microarray analyses (data from the NCBI Gene Expression Omnibus [37], accession number GSE20420) and Supplemental Table S1, it could be observed that genes necessary to activate respiratory genes and important for the diauxic transition, such as*YGP1*, *SPI1* and *GAC1*, and the transcription factor *ADR1*, were upregulated in Hcm1-overexpressed cells. Similarly, upregulation of *MSN2/4* and *GIS1* was observed when Hcm1 was overexpressed (Supplemental Table S1). Msn2/4 regulates expression of stress-responsive (STRE) genes while Gis1 induces transcription of postdiauxic shift (PDS) genes. These two transcription factors are located downstream of Rim15, a glucose-repressible kinase important in nutrient depletion [15] and also upregulated by Hcm1 (Supplemental Table S1). Thus, at stationary phase, cells became extremely resistant to oxidative and other stresses, being able to survive for weeks without nutrients [38].

The general metabolic response induced in Hcm1-overexpressed cells includes increasing expression of a variety of genes involved in i) high affinity glucose transport and hexokinases, ii) amino acid transport and mitochondrial metabolization of alternative energy sources, like proline and arginine, iii) NAD biosynthesis, and iv) stress resistance (Supplemental Fig. S2). Quantitative RT-PCR performed to validate the physiological role of Hcm1 *in vivo* showed that, in comparison to *Δhcm1* cells, WT cells presented higher induction levels of several such genes when nutrients became scarce (Fig. 3). To investigate whether Hcm1 responds either to decreased glucose or nitrogen levels, both Hcm1 protein levels and nuclear shift were measured. Both parameters increased when either glucose or nitrogen were limited, pointing to a general response of Hcm1 when nutrient levels decrease. The *in vivo* role of Hcm1 when nutrients decrease is further supported by its transcriptional activity, measured as the β-galactosidase activity in a strain carrying the known Hcm1 binding site of the *WHI5* promoter, fused to *LacZ*.

Nutrients are essential to the generation of cellular components and metabolites, but also fulfill regulatory functions, triggering signaling pathways. From the old concept of linear pathways acting in parallel, the actual picture points to a nutrient-dependent signaling network with extensive cross-talk at different levels. The results presented here suggest that Snf1 may act as the most important physiological regulator of Hcm1. Around 75% of *Δsnf1* cells have cytosolic Hcm1 localization, have problems dividing, and do not reach high cell densities. *In vitro* assays demonstrate that Hcm1 is a good substrate for this kinase. Snf1 is the central component of the main glucose repression pathway in yeast and is orthologous to the mammalian AMPK. In the presence of high levels of glucose, this serine/threonine kinase is inactivated through dephosphorylation by the protein

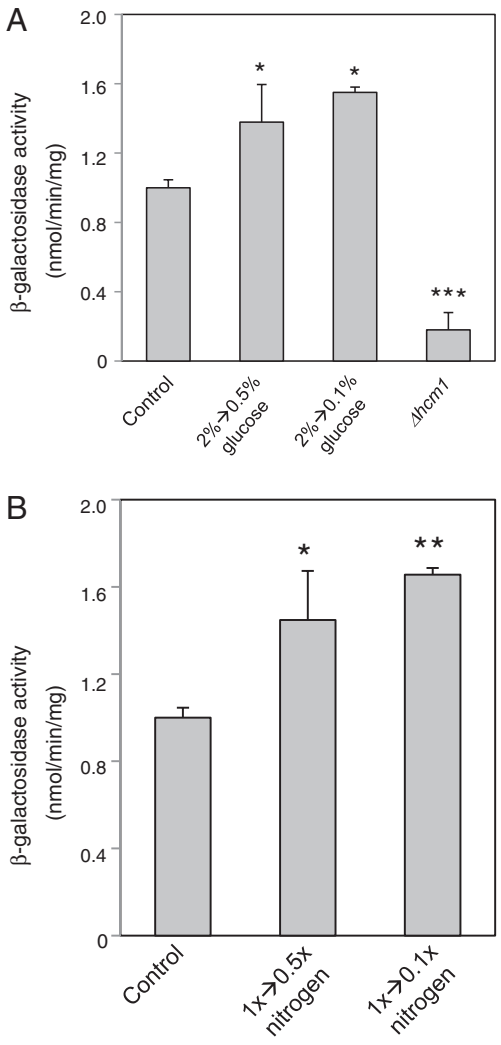

Fig. 5. Transcriptional activity of Hcm1 increases when either glucose or nitrogen content decreases. MJRC26 strain carrying the Hcm1-binding site from *WHI5* promoter, fused to LacZ and used as a reporter of Hcm1 transcriptional activity, was grown in SC medium (as described in Materials and methods) to $OD_{600}=0.5$. Cells were centrifuged, resuspended in new media with the amount of glucose or nitrogen indicated, and after 60 min incubation β-galactosidase activity was measured. β-galactosidase activity from MJRC27 strain (*Δhcm1* background) was used as a negative control. Activity is indicated as $nmol.min^{-1}.mg^{-1}$. Data are represented as means ± SD from three independent experiments. Statistical analysis was performed by comparison to control cells. $^{*}p<0.05$; $^{**}p<0.01$; $^{***}p<0.005$.

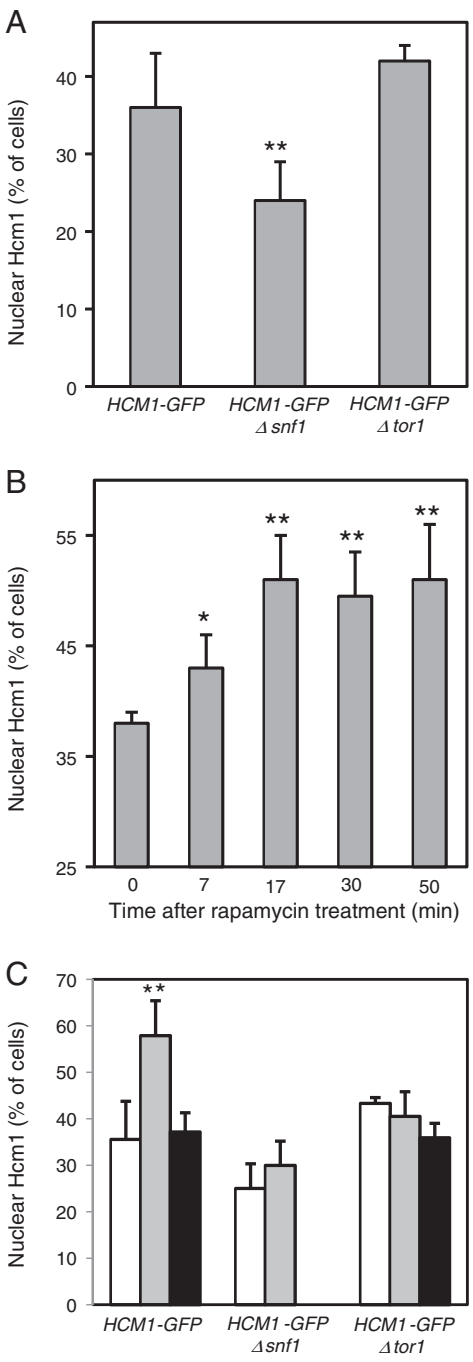

Fig. 6. Role of nutrient-sensory protein kinases in Hcm1 regulation. A. Cultures of WT (*HCM1-GFP*) and its derivative deletion strains *Δtor1* and *Δsnf1* were grown in YPD medium to $OD_{600}=0.5$ and analyzed for GFP fluorescence. Images were taken and percentage of cells showing nuclear Hcm1-GFP localization was quantified. Statistical analysis was performed by comparison to WT cells. B. *HCM1-GFP* cells were grown in YPD and analyzed for GFP fluorescence. Images were taken before and after 100 nM rapamycin addition and Hcm1-GFP localization analyzed. Statistical analysis was performed by comparison to control untreated cells. C. Cultures of WT (*HCM1-GFP*) and its derivative deletion strains *Δtor1* and *Δsnf1* were grown in YPD medium to $OD_{600}=0.5$ (white bars), $OD_{600}=3$ (gray bars) and $OD_{600}=7$ (black bars) and Hcm1-GFP nuclear localization was analyzed by fluorescence microscopy. Statistical analysis was performed by comparison to cells grown to $OD_{600}=0.5$. $^{*}p<0.05$; $^{**}p<0.01$.

phosphatase complex Glc7–Reg1 [39–41]. Inactivation of Snf1 by high glucose levels resulted in transcriptional repression of genes not needed during glucose fermentation. These effects are mainly due to the transcriptional repressor Mig1. The genes repressed by Mig1 encode for enzymes involved in the Krebs cycle, respiration, gluconeogenesis, and the uptake and metabolism of alternative carbon sources [14,42]. When glucose became scarce, ADP activates Snf1 by protecting the enzyme against dephosphorylation by Glc7 [43]. This requires increased interaction of Snf4 with the regulatory subunit of Snf1 and phosphorylation of Snf1 at Thre210, located at the catalytic domain. Three redundant upstream kinases –Elm1, Tos3, and Sak1 (formerly referred as Pak1)– can perform this phosphorylation [44]. In addition, relocalization of Snf1 has important effects on gene expression [15]. Activation of Snf1 by low glucose levels results in Mig1 phosphorylation and translocation of the repressor to the cytoplasm [31,45]. We showed that activation of Snf1 is detected as earlier as $OD_{600}=2$ showing a maximum activation around $OD_{600}=4$–5 (Fig. 2C). This implies that cells sense small decreases in nutrient levels and progressively change their metabolism to adapt to increasing nutrient scarcity. Phosphorylation of Hcm1 can be detected *in vivo* when cell extracts were prepared by a cell boiling method. Several bands can be observed at different points in the growth curve, supporting the hypothesis that Hcm1 is phosphorylated by several

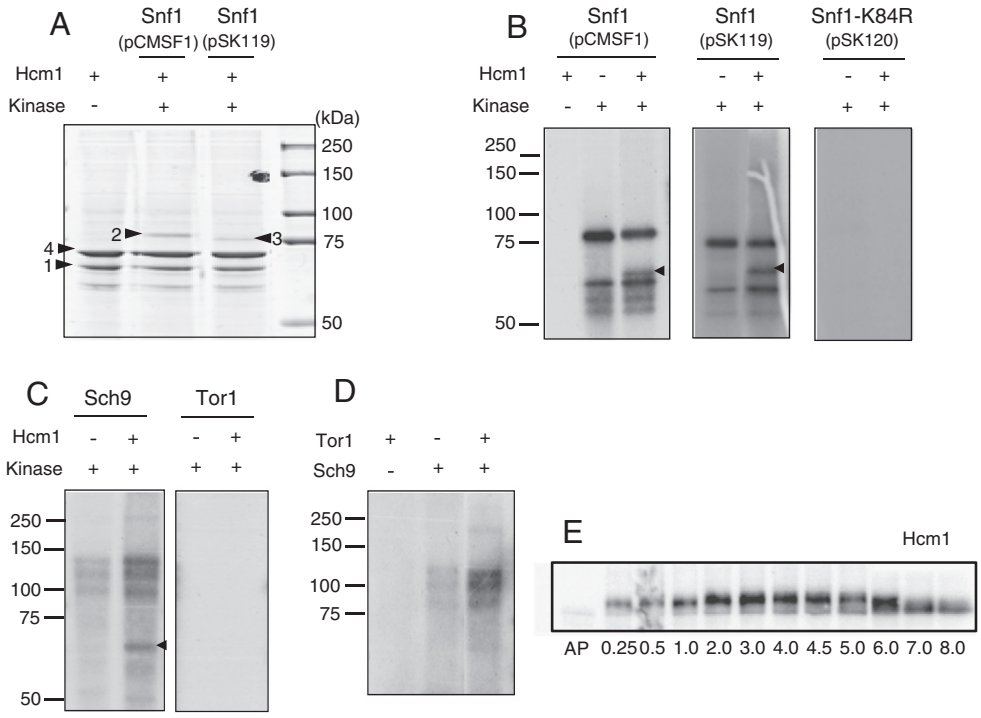

Fig. 7. Phosphorylation of Hcm1 by protein kinases. A. Purified recombinant Hcm1 alone or mixed with purified kinases were separated by SDS-PAGE and Coomassie brilliant blue stained. 1: Hcm1-His (Mw: 64.6 kDa); 2: Snf1-HA-His from pCMSF1 (Mw: 76.3 kDa); 3: HA-Snf1 from pSK119 (Mw: 75.3 kDa); 4: bifunctional polymyxin resistance protein ArnA, from *E. coli* (Mw: 74.3 kDa). B and C. Phosphorylation of Hcm1 by Snf1, Sch9, and Tor1 kinases was analyzed by detecting radioactivity of ^{32}P of [γ-^{32}P]ATP after SDS-PAGE electrophoresis. Arrowheads indicate phosphorylated Hcm1. B. Purified Hcm1 was incubated with [γ-^{32}P]ATP and active Snf1 (either from pCMSF1 and pSK119) or dead Snf1-K84R (from pSK120) for 45 min according to the Materials and methods and followed by SDS-PAGE electrophoresis. C. Purified Hcm1 was incubated with [γ-^{32}P]ATP and Sch9 or Tor1 for 45 min and followed by SDS-PAGE electrophoresis. D. Phosphorylation of Sch9 by Tor1 was analyzed. E. *HCM1-HA* cells were grown with YPD and Hcm1 levels were analyzed by western blot with anti-HA antibodies. Phosphorylation of Hcm1 can be detected when cell extract was obtained using the cell boiling procedure as described in Materials and methods. In the first lane (AP), cell extracts obtained by disruption with glass beads in phosphatase buffer were incubated with alkaline phosphatase (rAP, Roche) for 30 min to dephosphorylate Hcm1.

kinases at different sites. The fact that at $OD_{600} = 8$ the protein appears less phosphorylated and decreases its amount is in agreement with an early role on nutrient deficiency. Results obtained by *in vitro* assays suggest that active Snf1 phosphorylates Hcm1, stimulating its nuclear translocation and initiating the metabolic change described above. Thus, both Hcm1 and Mig1 would be Snf1 targets acting in metabolically opposite directions. Once Hcm1 translocates to the nucleus, this would induce a positive feedback loop, activating Snf1. This hypothesis is supported because *ELM1*, the Snf1-upstream kinase, is induced in *tetHCM1* cells and the phosphatase *GLC7* showed decreased expression levels (Table 3).

In addition to its primary role in response to nutrient stress, Snf1 has a role in cellular responses to other environmental stresses, including oxidative stress [19]. The activity of Msn2/4 and Hsf1, transcriptional activators involved in general stress responses, was shown to be modulated by Snf1 [46,47]. In the present study we observed that, when nutrients decrease, the induction of *HSP26* is highly dependent on Hcm1 (Fig. 3). The promoter of *HSP26* gene has a binding site for Hcm1 [12], suggesting a direct transcriptional regulation by the forkhead factor. Hsp26 is a small heat shock protein with chaperone activity strongly induced by several stresses, including nitrogen starvation, carbon starvation, and oxidative stress. Moreover, several genes involved in the response to stress are induced in cells overexpressing Hcm1 (Supplemental Table S1). Thus, Hcm1 activation by Snf1 would have a role in the well-known increased stress resistance when yeast cells begin to shift from fermentation to respiration [38,48,49].

In mammals, FoxO regulation is complex and has been extensively analyzed [2,36]. AMPK phosphorylates human FoxO3 at six regulatory sites activating its transcriptional activity. This phosphorylation does not affect the subcellular localization of FoxO3 [50]. However, nuclear translocation of FoxO3 has been described to be AMPK-dependent after prolonged inactivation of p38α [51]. AMPK activation by 5-aminoimidazole-4-carboxamide ribonucleotide (AIACAR) also promotes FoxO3 nuclear translocation and activation and reduces reactive oxygen species (ROS) levels [52]. Moreover, AMPK regulates FoxO activity by modulating other proteins, like SirT1. AMPK increases cellular NAD^+ levels, which enhance SirT1 activity and result in the deacetylation and activation of FoxO3 [53]. In yeast, Sir2 was described to regulate nuclear accumulation of Hcm1 upon oxidative stress [13], but whether Snf1 or another pathway is involved is not yet known.

Besides Snf1, other signaling pathways have a role as regulators of Hcm1. In this report we show that *Δtor1* cells showed slightly increased nuclear Hcm1 localization compared to WT cells at the early exponential phase ($OD_{600} = 0.5$). In addition, *Δtor1* cells did not show the transient translocation of Hcm1 to the nucleus when nutrients decreased ($OD_{600} = 3$). A possibility to explain the lack of response when nutrients decrease in a *Δtor1* mutant came from the described regulation of Snf1 by Tor1. Orlova and collaborators [54] demonstrated that Snf1 is negatively regulated by the rapamycin-sensitive Tor kinase, which plays essential roles in signaling nitrogen and amino acid availability. The authors showed that, upon nitrogen limitation, Snf1 is phosphorylated in a Tor1 dependent manner. In our context, perhaps lack of Hcm1 response when cells reached an $OD_{600} = 3$ is due to decreased activation of Snf1 by Tor1. In this context, nuclear Hcm1 import after rapamycin treatment supports the indirect role of the TORC1 pathway on Hcm1 regulation. Although TORC1 is regulated by the abundance and/or quality of the available carbon and nitrogen sources, glutamine appears to play a relevant role in its activation [55]. The nitrogen content affects Hcm1 localization and transcriptional activity. Shifting from high to low nitrogen levels induces Hcm1 activity. One possibility to explain how TORC1 signaling pathway regulates Hcm1 is through activation of Sch9 by phosphorylation. We observed that, at least *in vitro*, Tor1 does not phosphorylate Hcm1 directly, but phosphorylates Sch9 that, in turn, can phosphorylate Hcm1. Sch9 has been described to be directly

Table 3
mRNA levels of differentially expressed genes involved in nutrient limitation.

Gene	Microarrays[a]			RT-PCR[b]				Gene function[c]
	Δhcm1/ WT	*tetHCM1*/ WT	*tetHCM1*/ *tetHCM1* + doxy	*Δhcm1*/ WT	*tetHCM1*/ WT	*tetHCM1* + doxy/WT	*tetHCM1*/ *tetHCM1* + doxy	
AMPK pathway								
SNF1	1.03 ± 0.25	0.65 ± 0.09	1.22 ± 0.30					AMP-activated protein kinase; required for transcription of glucose-repressed genes, thermotolerance, sporulation, and peroxisome biogenesis.
ELM1	0.91 ± 0.09	1.62 ± 0.08	1.85 ± 0.10					Serine/threonine protein kinase that regulates cellular morphogenesis, septin behavior, and cytokinesis; required for the regulation of other kinases, including Snf1. Forms part of the bud neck ring.
GLC7	0.85 ± 0.12	0.91 ± 0.09	0.52 ± 0.08					Type 1 serine/threonine protein phosphatase catalytic subunit, involved in many processes (e.g., glycogen metabolism, sporulation, mitosis); accumulates at mating projections by interaction with Afr1p; interacts with many regulatory subunits.
REG1	0.80 ± 0.21	0.84 ± 0.08	0.75 ± 0.13					Regulatory subunit of type 1 protein phosphatase Glc7p, involved in negative regulation of glucose-repressible genes.
HXK2	1.30 ± 0.32	0.62 ± 0.10	0.63 ± 0.16					Hexokinase isoenzyme 2. Predominant HK during growth on glucose; functions in the nucleus to repress expression of *HXK1* and to induce expression of its own gene.
AKT/PKB pathway								
SCH9	0.82 ± 0.17	0.81 ± 0.20	0.72 ± 0.35	0.77	1.15	0.77	1.15	Protein kinase phosphorylated by Tor1p and required for TORC1-mediated regulation of ribosome biogenesis, translation initiation, and entry into G0 phase. Involved in transcriptional activation of osmostress-responsive genes. Regulates G1 progression, cAPK activity, and nitrogen activation of the FGM pathway. Integrates nutrient signals and stress signals to regulate lifespan; homologous to mammalian Akt/PKB.
TOR pathway								
TOR1	0.91 ± 0.20	0.89 ± 0.08	0.77 ± 0.13	1.04	0.87	1.04	0.87	PIK-related protein kinase and rapamycin target; subunit of TORC1.
TOR2	0.95 ± 0.05	0.90 ± 0.20	0.88 ± 0.22					PIK-related protein kinase and rapamycin target; subunit of TORC1.
LST8	0.99 ± 0.11	0.94 ± 0.18	0.59 ± 0.12	1.31	0.69	1.31	0.69	Component of the TOR signaling pathway; associates with both Tor1 and Tor2.
GAP1	0.6 ± 0.16	1.12 ± 0.12	2.6 ± 0.20					General amino acid permease; Gap1p senses the presence of amino acid substrates to regulate localization to the plasma membrane when needed.
TAT2	1.18 ± 0.15	0.87 ± 0.12	0.65 ± 0.27					High affinity tryptophan and tyrosine permease.
AUA1	1.45 ± 0.21	ND	0.25 ± 0.11					Protein required for the negative regulation by ammonia of Gap1p, which is a general amino acid permease.

[a] Microarray data is the average ± SD of two biological repeats.
[b] Quantitative RT-PCR data represents the average three technical repeats each with a variation lower than 10%.
[c] Gene function according to SGD [61].

phosphorylated by TORC1 on at least five residues, and these events are critical for Sch9 catalytic activity [23]. Sch9 has been described to function both in the cytoplasm and the nucleus, and in our context, phosphorylation of Hcm1 by Sch9 might induce nucleus export and/or cytoplasmic retention. In mammals, the regulatory role of FoxO by the insulin/PI3K/AKT pathway is the best studied [reviewed in 36]. In the presence of insulin, and as a consequence of AKT/PKB activation, FoxO1, 3 and 4 are phosphorylated at three evolutively conserved sites. The chaperone 14–3–3 has been identified as an important protein involved in the nuclear-cytoplasmic shuttling of FoxOs. Phosphorylation by AKT/PKB facilitates binding of FoxOs to the protein 14–3–3, enhancing nuclear export and decreasing nuclear entry [56,57]. Subsequently, AKT/PKB induces FoxO degradation by the ubiquitin–proteasome pathway.

As in the case of the AMPK pathway, there seems to be a feedback loop between Hcm1 activation and TORC1 inactivation. *LST8*, a component of TORC1, is downregulated in Hcm1-overexpressed cells and upregulated in *Δhcm1*, compared to the WT strain (Table 3). Expression of two genes downstream of the TORC1 pathway differs in *tetHCM1* cells: *TAT2* is downregulated, whereas *GAP1* is upregulated. Tat2 is a high-affinity tryptophan permease targeted to the plasma membrane under nutrient-rich conditions, but sorted to the vacuole for degradation when nitrogen sources are poor or limited. The opposite happens to Gap1, a general amino acid permease expressed when

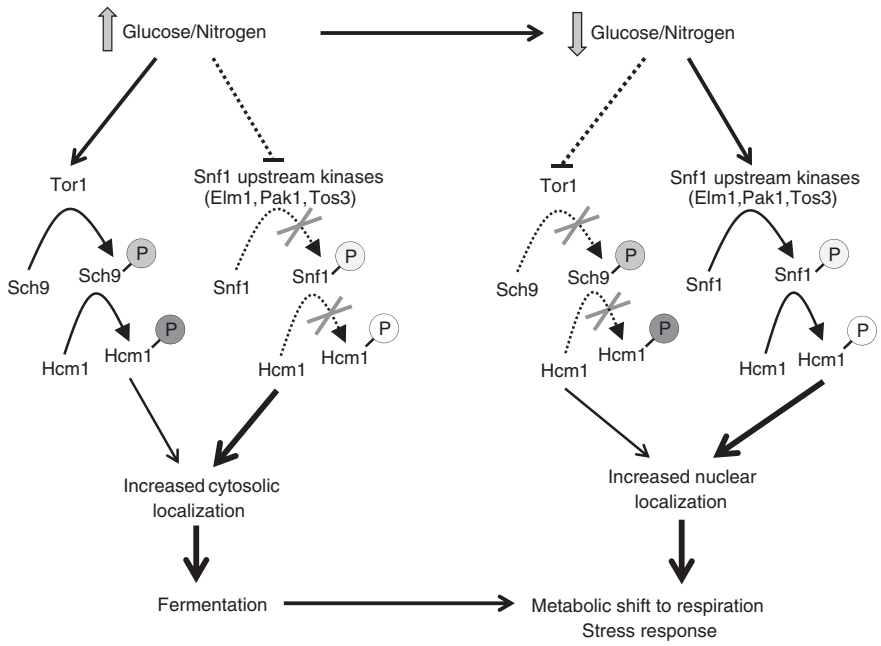

Fig. 8. Hcm1 acts as a downstream effector mainly of Snf1 pathway but also of Tor1/Sch9 pathway. In the presence of high glucose and nitrogen levels in the medium, the protein kinase Snf1 is inactivated and Tor1 becomes active and phosphorylates Sch9. Inactivation of the AMPK pathway and phosphorylation of Hcm1 by Sch9 results in increased cytosolic localization of Hcm1, decreasing its transcriptional activity. When nutrient levels drop, Snf1 is activated and Tor1 inactivated. Phosphorylation of Hcm1 by Snf1 induces nuclear translocation and transcriptional activation of Hcm1, which results in a shift to respiratory metabolism and oxidative stress resistance.

nitrogen sources are poor or limited [58,59]. Moreover, *AUA1*, a protein required for the negative regulation by ammonia of Gap1 [60] is downregulated. This report demonstrates that when nutrients start to decrease Hcm1 is upregulated and translocates transiently to the nucleus —probably as a result of phosphorylation by Snf1. Inside the nucleus, Hcm1 participated in the adaptation of cells to this new situation, being involved in the shift from fermentative to respiratory metabolism and inducing a stress response. The fact that Hcm1 activity achieves its maximum very early in the growth curve suggests that Hcm1 acts as a major nutrient regulator when nutrient limitation begins.

Supplementary data to this article can be found online at http://dx.doi.org/10.1016/j.bbamcr.2013.02.015.

Acknowledgements

We thank Roser Pané and Rosa Gómez for technical assistance. This work has been supported by grants BFU2010-17387 and CSD2007-20 Consolider Ingenio 2010 from the Ministerio de Ciencia e Innovación (Spain) and SGR2009-00196 from the Generalitat de Catalunya. M.J. Rodriguez-Colman is a recipient of a Ph.D. fellowship from the Ministerio de Ciencia e Innovación (Spain). We thank Elaine M. Lilly, Ph. D., for editing assistance.

References

[1] A. Van der Horst, B.M. Burgering, Stressing the role of FoxO proteins in lifespan and disease, Nature 8 (2007) 440–450.
[2] D.R. Calnan, A. Brunet, The FoxO code, Oncogene 27 (2008) 2276–2288.
[3] K.C. Arden, FOXO animal models reveal a variety of diverse roles for FOXO transcription factors, Oncogene 27 (2008) 2345–2350.
[4] K.E. Van der Vos, P.J. Coffer, FOXO-binding partners: it takes two to tango, Oncogene 27 (2008) 2289–2299.
[5] H. Daitoku, J. Sakamaki, A. Fukamizu, Regulation of FoxO transcription factors by acetylation and protein–protein interactions, Biochim. Biophys. Acta 1813 (2011) 1954–1960.
[6] K.H. Kaestner, W. Knochel, D.E. Martinez, Unified nomenclature for the winged helix/forkhead transcription factors, Genes Dev. 14 (2000) 142–146.
[7] P.C. Hollenhorst, M.E. Bose, M.R. Mielke, U. Müller, C.A. Fox, Forkhead genes in transcriptional silencing, cell morphology and the cell cycle. Overlapping and distinct functions for FKH1 and FKH2 in *Saccharomyces cerevisiae*, Genetics 54 (2000) 1533–1548.
[8] G. Zhu, P.T. Spellman, T. Volpe, P.O. Brown, D. Botstein, T.N. Davis, B. Futcher, Two yeast forkhead genes regulate the cell cycle and pseudohyphal growth, Nature 406 (2000) 90–94.
[9] S.D. Postnikoff, M.E. Malo, B. Wong, T.A. Harkness, The yeast forkhead transcription factors fkh1 and fkh2 regulate lifespan and stress response together with the anaphase-promoting complex, PLoS Genet. 8 (2012) e1002583.
[10] M. Kleinschmidt, R. Schulz, G.H. Braus, The yeast CPC2/ASC1 gene is regulated by the transcription factors Fhl1p and Ifh1p, Curr. Genet. 49 (2006) 218–228.
[11] C.E. Horak, N.M. Luscombe, J. Qian, P. Bertone, S. Piccirrillo, M. Gerstein, M. Snyder, Complex transcriptional circuitry at the G1/S transition in *Saccharomyces cerevisiae*, Genes Dev. 16 (2002) 3017–3033.
[12] T. Pramila, W. Wu, S. Miles, W.S. Noble, L.L. Breeden, The Forkhead transcription factor Hcm1 regulates chromosome segregation genes and fills the S-phase gap in the transcriptional circuitry of the cell cycle, Genes Dev. 20 (2006) 2266–2278.
[13] M.J. Rodriguez-Colman, G. Reverter-Branchat, M.A. Sorolla, J. Tamarit, J. Ros, E. Cabiscol, The forkhead transcription factor Hcm1 promotes mitochondrial biogenesis and stress resistance in yeast, J. Biol. Chem. 285 (2010) 37092–37101.
[14] J.M. Gancedo, Yeast carbon catabolite repression, Microbiol. Mol. Biol. Rev. 62 (1998) 334–361.
[15] B. Smets, R. Ghillebert, P. De Snijder, M. Binda, E. Swinnen, C. De Virgilio, J. Winderickx, Life in the midst of scarcity: adaptations to nutrient availability in *Saccharomyces cerevisiae*, Curr. Genet. 56 (2010) 1–32.
[16] K. Hedbacker, M. Carlson, SNF1/AMPK pathways in yeast, Front. Biosci. 13 (2008) 2408–2420.
[17] M. Carlson, B.C. Osmond, D. Botstein, Mutants of yeast defective in sucrose utilization, Genetics 98 (1981) 25–40.
[18] K. Ashrafi, S.S. Lin, J.K. Manchester, J.I. Gordon, Sip2p and its partner Snf1p kinase affect aging in *S. cerevisiae*, Genes Dev. 14 (2000) 1872–1885.
[19] S.P. Hong, M. Carlson, Regulation of Snf1 protein kinase to environmental stresses, J. Biol. Chem. 282 (2007) 16838–16845.
[20] M.N. Hall, The TOR signalling pathway and growth control in yeast, Biochem. Soc. Trans. 24 (1996) 234–239.
[21] Y. Wei, X.F. Zheng, Nutritional control of cell growth via TOR signaling in budding yeast, Methods Mol. Biol. 759 (2011) 307–319.
[22] J.R. Rohde, R. Bastidas, R. Puria, M.E. Cardenas, Nutritional control via Tor signaling in *Saccharomyces cerevisiae*, Curr. Opin. Microbiol. 11 (2008) 153–160.
[23] J. Urban, A. Soulard, A. Huber, S. Lippman, D. Mukhopadhyay, O. Deloche, V. Wanke, D. Anrather, G. Ammerer, H. Riezman, J.R. Broach, C. De Virgilio, M.N. Hall, R. Loewith, Sch9 is a major target of TORC1 in *Saccharomyces cerevisiae*, Mol. Cell. 26 (2007) 663–674.
[24] A. Huber, B. Bodenmiller, A. Uotila, M. Stahl, S. Wanka, B. Gerrits, R. Aebersold, R. Loewith, Characterization of the rapamycin-sensitive phosphoproteome reveals that Sch9 is a central coordinator of protein synthesis, Genes Dev. 23 (2009) 1929–1943.
[25] F.M. Ausubel, R. Brent, E.E. Kingston, D.D. Moore, J.G. Seidman, J.A. Smith, K. Struhl, Current Protocols in Molecular Biology, John Wiley and Sons Inc., Hoboken, NJ, 1987.
[26] C. Gallego, E. Garí, N. Colomina, E. Herrero, M. Aldea, The Cln3 cyclin is down-regulated by translational repression and degradation during the G1 arrest caused by nitrogen deprivation in budding yeast, EMBO J. 16 (1997) 7196–7206.

[27] A.L. Goldstein, J.H. McCusker, Three new dominant drug resistance cassettes for gene disruption in *Saccharomyces cerevisiae*, Yeast 15 (1999) 1541–1553.
[28] F. Sherman, Getting started with yeast, Methods Enzymol. 350 (2002) 3–41.
[29] E. Garí, L. Piedrafita, M. Aldea, E. Herrero, A set of vectors with a tetracycline-regulatable promoter system for modulated gene expression in *Saccharomyces cerevisiae*, Yeast 13 (1997) 837–848.
[30] G. Bellí, E. Garí, M. Aldea, E. Herrero, Functional analysis of yeast essential genes using a promoter-substitution cassette and the tetracycline-regulatable dual expression system, Yeast 14 (1998) 1127–1138.
[31] M.A. Treitel, S. Kuchin, M. Carlson, Snf1 protein kinase regulates phosphorylation of the Mig1 repressor in *Saccharomyces cerevisiae*, Mol. Cell. Biol. 18 (1998) 6273–6280.
[32] L. Guarente, Yeast promoters and lacZ fusions designed to study expression of cloned genes in yeast, Methods Enzymol. 101 (1983) 181–191.
[33] G. Reverter-Branchat, E. Cabiscol, J. Tamarit, M.A. Sorolla, M. Angeles de la Torre, J. Ros, Chronological and replicative life-span extension in *Saccharomyces cerevisiae* by increased dosage of alcohol dehydrogenase 1, Microbiology 153 (2007) 3667–3676.
[34] M. Orlova, L. Barret, S. Kuchin, Detection of endogenous Snf1 and its activation state: application to *Saccharomyces* and *Candida* species, Yeast 25 (2008) 745–754.
[35] L. Viladevall, R. Serrano, A. Ruiz, G. Domenech, J. Giraldo, A. Barceló, J. Ariño, Characterization of the calcium-mediated response to alkaline stress in *Saccharomyces cerevisiae*, J. Biol. Chem. 279 (2004) 43614–43624.
[36] Y. Zhao, Y. Wang, W.G. Zhu, Applications of post-translational modifications of FoxO family proteins in biological functions, J. Mol. Cell Biol. 3 (2011) 276–282.
[37] R. Edgar, M. Domrachev, A.E. Lash, Gene Expression Omnibus: NCBI gene expression and hybridization array data repository, Nucleic Acids Res. 30 (2002) 207–210.
[38] G. Reverter-Branchat, E. Cabiscol, J. Tamarit, J. Ros, Oxidative damage to specific proteins in replicative and chronological-aged *Saccharomyces cerevisiae*: common targets and prevention by calorie restriction, J. Biol. Chem. 279 (2004) 31983–31989.
[39] K. Ludin, R. Jiang, M. Carlson, Glucose-regulated interaction of a regulatory subunit of protein phosphatase 1 with the Snf1 protein kinase in *Saccharomyces cerevisiae*, Proc. Natl. Acad. Sci. U. S. A. 95 (1998) 6245–6250.
[40] P. Sanz, G.R. Alms, T.A. Haystead, M. Carlson, Regulatory interactions between the Reg1-Glc7 protein phosphatase and the Snf1 protein kinase, Mol. Cell. Biol. 20 (2000) 1321–1328.
[41] R.R. McCartney, M.C. Schmidt, Regulation of Snf1 kinase. Activation requires phosphorylation of threonine 210 by an upstream kinase as well as a distinct step mediated by the Snf4 subunit, J. Biol. Chem. 276 (2001) 36460–36466.
[42] H. Ronne, Glucose repression in fungi, Trends Genet. 11 (1995) 12–17.
[43] F.V. Mayer, R. Heath, E. Underwood, M.J. Sanders, D. Carmena, R.R. McCartney, F.C. Leiper, B. Xiao, C. Jing, P.A. Walker, L.F. Haire, R. Ogrodowicz, S.R. Martin, M.C. Schmidt, S.J. Gamblin, D. Carling, ADP regulates Snf1 the *Saccharomyces cerevisiae* homolog of AMP-activated protein kinase, Cell Metab. 14 (2011) 707–714.
[44] S.P. Hong, F.C. Leiper, A. Woods, D. Carling, M. Carlson, Activation of yeast Snf1 and mammalian AMP-activated protein kinase by upstream kinases, Proc. Natl. Acad. Sci. U. S. A. 100 (2003) 8839–8843.
[45] M. Papamichos-Chronakis, T. Gligoris, D. Tzamarias, The Snf1 kinase controls glucose repression in yeast by modulating interactions between the Mig1 repressor and the Cyc8-Tup1 co-repressor, EMBO Rep. 5 (2004) 368–372.
[46] P.G. Bertram, J.H. Choi, J. Carvalho, T.F. Chan, W. Ai, X.F. Zheng, Convergence of TOR-nitrogen and Snf1-glucose signaling pathways onto Gln3, Mol. Cell. Biol. 22 (2002) 1246–1252.
[47] J.S. Hahn, D.J. Thiele, Activation of the *Saccharomyces cerevisiae* heat shock transcription factor under glucose starvation conditions by Snf1 protein kinase, J. Biol. Chem. 279 (2004) 5169–5176.
[48] M. Werner-Washburne, E. Braun, G.C. Johnston, R.A. Singer, Stationary phase in the yeast *Saccharomyces cerevisiae*, Microbiol. Rev. 57 (1993) 383–401.
[49] D.W. Stephen, S.L. Rivers, D.J. Jamieson, The role of the YAP1 and YAP2 genes in the regulation of the adaptive oxidative stress responses of *Saccharomyces cerevisiae*, Mol. Microbiol. 16 (1995) 415–423.
[50] E.L. Greer, M.R. Banko, A. Brunet, AMP-activated protein kinase and FoxO transcription factors in dietary restriction-induced longevity, Ann. N. Y. Acad. Sci. 1170 (2009) 688–692.
[51] F. Chiacchiera, A. Matrone, E. Ferrari, G. Ingravallo, G. Lo Sasso, S. Murzilli, M. Petruzzelli, L. Salvatore, A. Moschetta, C. Simone, p38alpha blockade inhibits colorectal cancer growth in vivo by inducing a switch from HIF1alpha- to FoxO-dependent transcription, Cell Death Differ. 16 (2009) 1203–1214.
[52] X.N. Li, J. Song, L. Zhang, S.A. LeMaire, X. Hou, C. Zhang, J.S. Coselli, L. Chen, X.L. Wang, Y. Zhang, Y.H. Shen, Activation of AMPK-FOXO3 pathway reduces fatty acid-induced increase in intracellular reactive oxygen species by upregulating glutaredoxin, Diabetes 58 (2009) 2246–2257.
[53] C. Cantó, Z. Gerhart-Hines, J.N. Feige, M. Lagouge, L. Noriega, J.C. Milne, P.J. Elliott, P. Puigserver, J. Auwerx, AMPK regulates energy expenditure by modulating NAD^+ metabolism and SIRT1 activity, Nature 458 (2009) 1056–1060.
[54] M. Orlova, E. Kanter, D. Krakovich, S. Kuchin, Nitrogen availability and TOR regulate the Snf1 protein kinase in *Saccharomyces cerevisiae*, Eukaryot. Cell 5 (2006) 1831–1837.
[55] J.L. Crespo, T. Powers, B. Fowler, M.N. Hall, The TOR-controlled transcription activators GLN3, RTG1, and RTG3 are regulated in response to intracellular levels of glutamine, Proc. Natl. Acad. Sci. U. S. A. 99 (2002) 6784–6789.
[56] A. Brunet, F. Kanai, J. Stehn, J. Xu, D. Sarbassova, J.V. Frangioni, S.N. Dalal, J.A. DeCaprio, M.E. Greenberg, M.B. Yaffe, 14–3–3 transits to the nucleus and participates in dynamic nucleocytoplasmic transport, J. Cell Biol. 156 (2002) 817–828.
[57] V. Obsilova, J. Vecer, P. Herman, A. Pabianova, M. Sulc, J. Teisinger, E. Boura, T. Obsil, 14–3–3 protein interacts with nuclear localization sequence of forkhead transcription factor FoxO4, Biochemistry 44 (2005) 11608–11617.
[58] K.J. Roberg, N. Rowley, C.A. Kaiser, Physiological regulation of membrane protein sorting late in the secretory pathway of *Saccharomyces cerevisiae*, J. Cell Biol. 137 (1997) 1469–1482.
[59] T. Beck, M.N. Hall, The TOR signalling pathway controls nuclear localization of nutrient-regulated transcription factors, Nature 402 (1999) 689–692.
[60] V. Sophianopoulou, G. Diallinas, AUA1, a gene involved in ammonia regulation of amino acid transport in *Saccharomyces cerevisiae*, Mol. Microbiol. 8 (1993) 167–178.
[61] H.W. Mewes, D. Frishman, C. Gruber, B. Geier, D. Haase, A. Kaps, K. Lemcke, G. Mannhaupt, F. Pfeiffer, C. Schuller, S. Stocker, B. Weil, MIPS: a database for genomes and protein sequences, Nucleic Acids Res. 28 (2000) 37–40.